ORIGINAL ARTICLE

Earth system models for regional environmental management of red tide: Prospects and limitations of current generation models and next generation development

Ahmed S. Elshall[1] · Ming Ye[1] · Sven A. Kranz[1] · Julie Harrington[2] · Xiaojuan Yang[3] · Yongshan Wan[4] · Mathew Maltrud[5]

Abstract

Earth system models (ESMs) serve as a unique research infrastructure for quality climate services, yet their application for environmental management at regional scale has not yet been fully explored. The unprecedented resolution and model fidelity of the Coupled Model Intercomparison Project Phase 6 (CMIP6) simulations, especially of the High-Resolution Model Intercomparison Project (HighResMIP) focusing on regional phenomena, offer opportunities for such applications. This article presents the first venture into using the HighResMIP simulations to tackle a regional environmental issue, the Florida Red Tide. This is a harmful algae bloom caused by the dinoflagellate *Karenia brevis,* a toxic single-celled microscopic protist. We use CMIP6 historical simulations to establish a causal agreement between the position of Loop Current, a warm ocean current that moves into the Gulf of Mexico, and the occurrence of *K. brevis* blooms on the Western Florida shelf. Results show that the high-resolution ESMs are capable of simulating the phenomena of interest (i.e., Loop Current) at the regional spatial scale with generally adequate data-model agreement in the context of the relation between Loop Current and red tide. We use this case study to elaborate on the prospects and limitations of using publicly available CMIP data for regional environmental management. We highlight the current gaps and the developmental needs for the next generation ESMs, and discuss the role of stakeholder participation in future ESMs development to facilitate the translation of scientific understanding to better inform decision-making of regional environmental management.

Keywords Climate models and Earth system models · Harmful algal blooms · Red tide · Regional environmental management · Model validation · Western Florida Shelf at the Gulf of Mexico

Introduction

Earth system modeling lends a great potential for supporting regional environmental management (Ward et al. 2020; Dixon et al. 2021). Earth system modeling is evolving as an unprecedent research infrastructure that provides quality Earth system data and climate services for the society (Joussaume et al. 2017; Roberts et al. 2018b; Fiedler et al. 2021). For example, the publicly available data of the Coupled Model Intercomparison Project (CMIP) projects provide diverse climate services in water, agriculture, energy, and health sectors (Ilori and Balogun 2021; Usta et al. 2021; Ahmed 2021). Global climate models (GCMs) mainly simulate the physical atmospheric and oceanic processes with generally predetermined inputs of atmospheric composition. Earth system models (ESMs) reach far beyond GCMs by including explicit representation of biogeochemical

✉ Ming Ye
  mye@fsu.edu

1 Department of Earth, Ocean, and Atmospheric Science, Florida State University, Tallahassee, FL, USA

2 Center for Economic Forecasting and Analysis, Florida State University, Tallahassee, FL, USA

3 Environmental Sciences Division and Climate Change Science Institute, Oak Ridge National Laboratory, Oak Ridge, TN, USA

4 Center for Environmental Measurement and Modeling, United States Environmental Protection Agency, Gulf Breeze, FL, USA

5 Fluid Dynamics and Solid Mechanics Group, Los Alamos National Laboratory, Los Alamos, NM, USA

processes and their interactions with the physical climate. Accordingly, ESMs can better explore the human impacts on the Earth systems through coupled representations of human activities with the physics and biogeochemistry of the atmosphere, ocean, land, rivers, and cryosphere. Using ESMs we can explore and understand how Earth systems respond to natural and anthropogenic forcings, while assessing future climate changes and mitigation plans (Eyring et al. 2019). Thus, ESMs have the potential to serve as a unique interdisciplinary research infrastructure for regional environmental management.

Coupled Model Intercomparison Project Phase Six (CMIP6) offers avenues for regional environmental services. ESMs have been utilizable for regional environmental management through coupled regional ESMs such as the regionally coupled atmosphere-ocean-sea ice-marine biogeochemistry model (ROM, Sein et al 2015) and the Earth system regional climate model (RegCM-ES, Reale et al 2020). These regional ESMs include the same components as a global ESM, but cover a specific area with boundary conditions provided by global ESMs, or observation data. However, the compatibility across different model components is often restricted (Giorgi and Gao 2018), and there are often large uncertainties associated with the boundary conditions (Adachi and Tomita 2020). As such, coupled regional ESMs have been applied only to limited regional settings (Giorgi and Gao 2018). Yet out of the pressure to expand the scope of modeling in climate science, the CMIP6 became larger and more extensive in scope (Eyring et al. 2016). For example, CMIP6 endorsed a High-Resolution Model Intercomparison Project (HighResMIP, Haarsma et al. 2016) allowing ESMs with variable fine scale-grid resolution to focus on regional phenomena. This new generation of advanced high-resolution Earth system models (HR-ESMs) with improved horizontal resolution and process representation, particularly at the regional scale with unprecedented fidelity, enhances our confidence in predictions and projections (Roberts et al. 2018b). While these high-resolution models have very high computational cost, the data of these CMIP model runs are publicly available. HR-ESMs, that have nominal resolution of 25 km or less as being evaluated by CMIP6, go far beyond the standard low-resolution Earth system models (LR-ESMs) such as most of the simulations of CMIP5 and CMIP6 DECK historical experiment, which has a nominal resolution of 100 km. In addition, the Coordinated Regional Downscaling Experiment (CORDEX) uses CMIP outputs and provides, for selected regions, dynamically downscaled climate change experiments (Gutowski Jr. et al. 2016; Gutowski et al. 2020). This unprecedented resolution and model fidelity result in improved simulation of Earth processes that are of growing interest to societal decision-making. Accordingly, HR-ESMs may serve as a more reliable tool for assessing smaller-scale

phenomena such as tropical cyclones (Jiaxiang et al. 2020), climate extremes such as heatwaves and heavy precipitation (Iles et al. 2020), costal processes (Ward et al. 2020), coral reef conservation (Dixon et al. 2021), and regional ocean currents (Le et al. 2020).

This study discusses the potential use of ESMs for regional environmental management using the Florida red tide as a case study. Red tides are worldwide occurrences of intense harmful algae blooms (Tian and An 2013; Wen et al. 2013; Xu et al. 2014; Liu and Fang 2017). The Florida red tide is composed of mixotrophic dinoflagellate, *K. brevis*. These microscopic protists occur regularly along the West Florida Shelf and cause substantial environmental and socioeconomic damage. This includes impacts on human health (e.g., respiratory, skin, and eye irritation), fisheries (e.g., massive fish kills, and shellfish poisoning), ecosystem services (e.g., harming sea turtles, marine mammals, and birds), tourism (e.g., hotels, and restaurants), recreational activities, and local small business. The occurrence of red tides in the Gulf of Mexico may involve multiple system processes, including land-to-ocean nutrient and sediment transport from rivers and submarine groundwater discharge, ocean currents and upwelling, ocean biogeochemical processes, African Sahara dust, wind direction, and tropical cyclones (Brand and Compton 2007). Many of the physical and biogeochemical processes that are related to the occurrence of red tide can be simulated ESMs as discussed in "ESMs for regional environmental management" section. Accordingly, this research direction aims at using ESMs to understand the impact of climate changes on red tide frequency, and accordingly assess the environmental and socioeconomic impacts of red tide under different Shared Socioeconomic Pathways (SSPs, Riahi et al. 2017) of the CMIP6.

Given the above general research direction, here we focus on Loop Current, a regional ocean current in the Gulf of Mexico, which is particularly an important factor for predicting red tide occurrences (Weisberg et al. 2014; Maze et al. 2015; Liu et al. 2016b). The main objective of this manuscript is to present this case study to serve as an example to discuss the prospects and limitations of the current generation of CMIP6 and next generation development of ESMs for red tide management. In other words, we highlight the current modeling gaps and future research directions of ESMs as a useful tool for providing regional environmental management services.

Methods

Red tide hypothesis and data

A current working hypothesis of the occurrence of red tide in the West Florida Shelf is based on the position of the

Loop Current and its eddies (Perkins 2019) such that the Loop Current position can be "the first definitive predictor of bloom possibility" (Maze et al. 2015). The Loop Current and its eddies can be easily detected from sea surface height variability (Weisberg et al. 2014; Maze et al. 2015). Maze et al. (2015) showed that the differences in the Loop Current's position between periods of large blooms and no bloom are statistically significant such that a northern Loop Current (LCN) position (Fig. 1a) penetrating through the Gulf of Mexico is a necessary condition for a large red tide bloom to occur. In other words, there is no large bloom for southern Loop Current (LCS) position (Fig. 1b), while there could be a large bloom or no bloom for LCN (Fig. 1a). Similar to the definition of Maze et al. (2015), we defined a large bloom as an event with the cell count exceeding 1×10^5 cells/L for ten or more successive days without a gap of more than five consecutive days, or 20% of the bloom length in the study area (Fig. 1a). The *K. brevis* cell count data used in this study are from the harmful algal bloom database of the Fish and Wildlife Research Institute at the Florida Fish and Wildlife Conservation Commission (FWRI 2020). For the analysis period of 22 years from 1993 to 2015, there were 15 periods of large blooms, and 29 periods with no bloom given a 6-month period length.

Reanalysis data

The Loop Current can be identified from altimetry reanalysis data as an area with sea surface height above geoid (CMIP variable: zos) higher than the surrounding waters. We use the global-reanalysis-phy-001–030 monthly product of Copernicus Marine Environment Monitoring Service (CMEMS), a

global ocean eddy-resolving reanalysis covering the altimetry from 1993 to 2015 and onward with approximatively 8 km horizontal resolution (Drévillon et al. 2018; Fernandez and Lellouche 2018). Following Maze et al. (2015), the difference between the mean altimetry height along the two segments of the 300 m isobath (Fig. 1b) is used as a proxy for the Loop Current position (Appendix) such that positive and negative difference between the north and south segments indicates LCN (Fig. 1a) and LCS (Fig. 1b), respectively.

Earth system model data

We use multi-model ensemble of HR-ESMs with six ensemble members as shown in Table 1. For comparison, we use an ensemble of LR-ESMs with two ensemble members (i.e., EC-Earth3P and E3SM-1–0). The members are from both CMIP6 historical experiment (Eyring et al. 2016) and hist-1950 experiment (Haarsma et al. 2016). These are two sibling experiments that use historical forcings (e.g., historical greenhouse gases concentrations, solar forcing, etc.) of recent past until 2015. To reduce computational cost, the hist-1950 experiment starts from 1950 with initial conditions from the spin-up 1950 run. The historical experiment starts from 1850, initialized from any point early enough in the pre-industrial control run. Each member can have multiple runs with perturbed realizations (r), initializations (1), physics (p), and forcings (f) as shown in Table 1. For example, $r(1-6)$ of ECMWF-IFS-HR means six runs of six perturbed realizations. The HR-ESMs have an ocean nominal resolution ranging from 8 to 25 km. The two last digits of HadGEM3-GC31-HH/HM/MM refer to the atmosphere and ocean, respectively, each with high (H)
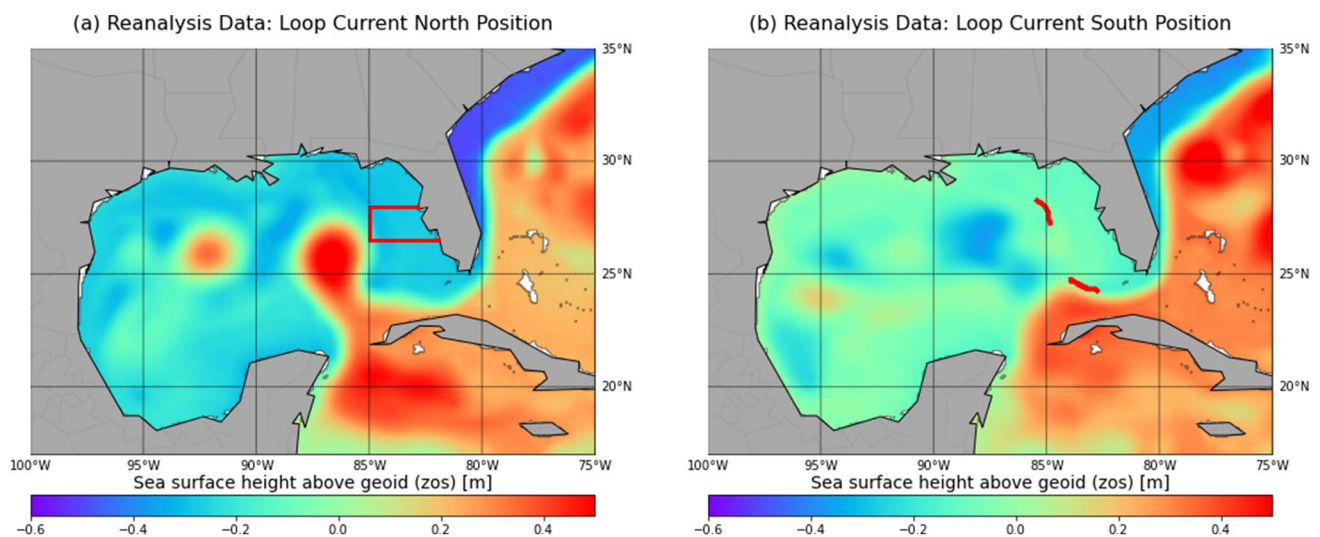

Fig. 1 Reanalysis data of sea surface height above geoid (zos) [m] reveal (**a**) LCN and (**b**) LCS. Two red segments along the 300 m isobath in (**b**) are used to determine Loop Current position, and the red box in (**a**) shows the area where red tide blooms are considered by Maze et al. (2015) and this study

Table 1 ESMs models used in this study consisting of six HR-ESMs (i.e., ocean model resolution of less than or equal 25 km) and two LR-ESMs

Model	Institution, location	Experiment	Model runs	Ocean grid	Ocean model resolution
ECMWF-IFS-HR (Roberts et al. 2018a)	ECMWF, Europe	hist-1950	r(1–6)i1p1f1	ORCA025	25 km nominal resolution
ECMWF-IFS-MR (Roberts et al. 2018a)	ECMWF, Europe	hist-1950	r(1–3)i1p1f1	ORCA025	25 km nominal resolution
HadGEM3-GC31-HH (Roberts et al. 2019)	NERC, UK	hist-1950	r1i1p1f1	ORCA12	8 km nominal resolution
HadGEM3-GC31-HM (Roberts et al. 2019)	MOHC-NERC, UK	hist-1950	r(1–3)i1p1f1	ORCA025	25 km nominal resolution
HadGEM3-GC31-MM (Roberts et al. 2019)	MOHC, UK	hist-1950	r1i(1–3)p1f1	ORCA025	25 km nominal resolution
HadGEM3-GC31-MM (Roberts et al. 2019)	MOHC, UK	Historical	r(1–4)i1p1f3	ORCA025	25 km nominal resolution
EC-Earth3P (Haarsma et al. 2020)	EC-Earth Consortium, Europe	hist-1950	r(1–3)i1p2f1	ORCA1	~1° (110 km grid spacing)
E3SM-1–0 (Golaz et al. 2019)	DOE-E3SM-Project, USA	Historical	r(1–5)i1p1f1	EC60to30	60 km mid-latitudes and 30 km equator and poles

or medium (M) resolutions. For LR-ESMs, E3SM-1–0 has variable ocean resolution of 30–60 km from the pole to the equator, and EC-Earth3P has a nominal ocean resolution of 1° (about 100 km).

Model validation

We investigate the agreement between model simulations and reanalysis data with respect to Loop Current position, and accordingly the possibility of large bloom occurrence following the empirical relation of Maze et al. (2015). To validate ESMs for this purpose, we identified three basic tasks with evolving difficulties. The first task is simulating the phenomena of interest at the regional spatial scale, which is the Loop Current in this case. The second task is to provide adequate estimation of the frequency of an oscillating event over the simulation period. This is achieved in this study by validating the frequency of LCN and LCS from model simulation with reanalysis data. This validation task is particularly important as the main purpose of this research direction is to understand the future frequency of red tide under different SSPs of CMIP6. Simulating the regional physical phenomena of interest (e.g., Loop Current) with an accurate frequency of oscillation are among the important steps toward this purpose along with the other steps that are presented in the discussion section. The third validation task is to examine the temporal agreement of Loop Current positions between model and reanalysis data.

Results and discussion

Loop current position simulation

The first task is to validate whether the models can simulate LCN and LCS positions. High-resolution eddy-permitting grids of HR-ESMs meet this modeling need as demonstrated by Fig. 2, which shows a snapshot comparison of the simulated sea surface height above geoid (variable: zos) from a low-resolution eddy closure EC60to30 mesh, and the high-resolution ORCA12 grid. Fig 2a shows that the low-resolution mesh cannot simulate LCN, whereas Fig. 2b indicates that the high-resolution ORCA12 grid resolves mesoscale eddies. Compared with LR-ESMs, HR-ESMs not only have a finer horizontal resolution, but also improved process description as reflected by the ocean grid in HR-ESMs. The low-resolution EC60to30 grid of E3SM-1–0, which is an eddy closure (EC) grid, is not expected to resolve the regional spatial phenomena of interest, but rather to produce global or regional average. This is mainly because low-resolution grids (e.g., EC60to30 of E3SM-1–0 and ORCA1 of EC-Earth3P in Table 1) require global parametrization of mesoscale eddies, rather than explicitly resolving mesoscale eddies and boundary currents. By contrast, high-resolution eddy-permitting grids (e.g., ORCA12 and ORCA025 in Table 1) do not require ocean eddy flux parameterization.

In this study, we are not arguing that global ESMs can replace regional models (e.g., the Gulf of Mexico HYCOM
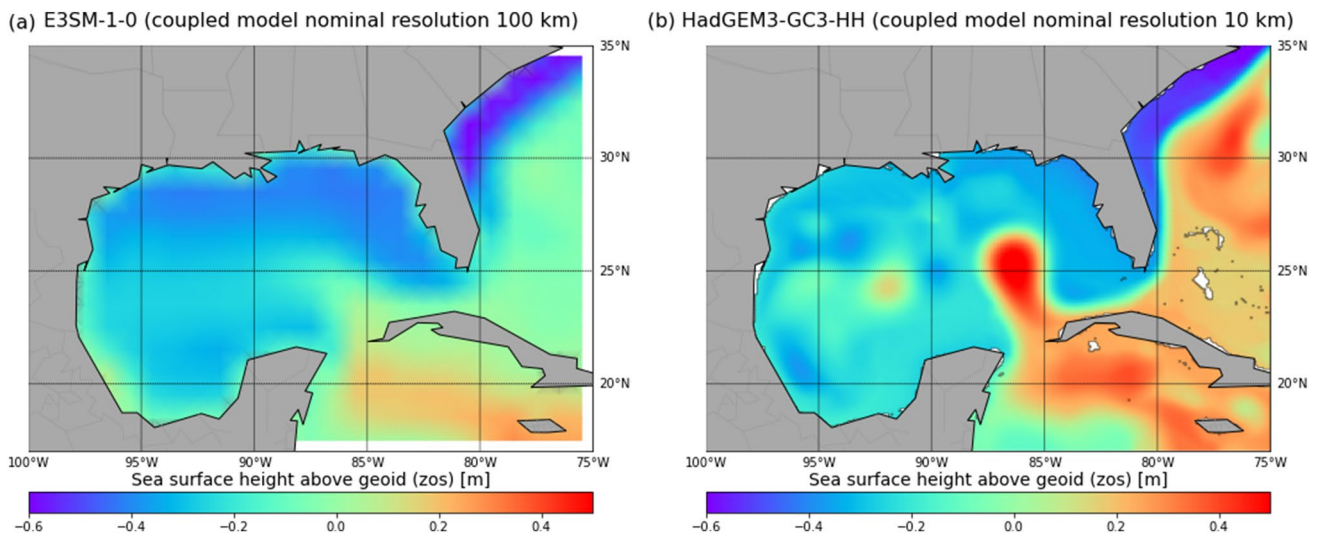
Fig. 2 A snapshot (March 2010) of sea surface height above geoid (zos) [m] simulated using a (**a**) LR-ESM, and (**b**) HR-ESM with nominal resolution of 100 km and 10 km, respectively

by the HYCOM Consortium) in accurately simulating the Loop Current and eddy positions. The Loop Current has a chaotic and random cycle with the average period being around one cycle every 8–18 months (Sturges and Evans 1983; Maze et al. 2015). The objective of this work is neither to accurately represent the shape of the Loop Current and its anticyclonic ring, nor to precisely simulate the time of Loop Current occurrence, which are even challenging tasks for regional models. The object of this research direction is to understand assess the validity of ESMs in regional environmental management. The specific objective of this study is model validation given the criteria of Maze et al. (2015) that is based Loop Current frequency.

Frequency of loop current position

The second validation task is related to event frequency, which is adequately estimated by the HR-ESMs ensemble. We plot the time series of the Loop Current position as inferred from the reanalysis data against occurrence of large blooms (Fig. 3a). For the study period of 22 years with 6 month interval length, there is a total of 44 intervals. For the reanalysis data, the LCN count is 32, and the LCS count is 12 (Eqs. A2–A4). The higher frequency of LCN than LCS is expected. This frequency ratio between LCS and LCN of 0.375 (i.e., 12/32) is very similar to that of Maze et al (2015), which is 0.364 given their study period from 1993 to 2007 and their reanalysis product (Eq.A2–A4). Additionally,

Fig. 3a indicates that no large blooms are associated with LCS (i.e., zos anomaly less than 0). This is consistent with the findings of Maze et al. (2015) that for LCS no large bloom occurs, and that LCN is a necessary condition for large bloom to occur.

To evaluate to what degree HR-ESMs can simulate the reanalysis data, the HR-ESMs predictive performance is shown in Fig. 3b, and the results are summarized in Table 2. A comparison between HR-ESMs and LR-ESMs with respect to frequency of an event and temporal agreement is summarized in Table 2. The LCN frequency over the study period is reasonably reproduced by HR-ESMs multi-model ensemble that has a frequency of 35 compared to 32 for the reanalysis data (Eqs. A2–A4). The best single-model ensemble ECMWF-IFS-MR, which has three repeated runs $r(1–3)i1p1f1$ as shown in Table 1, has a LCN frequency of 33 that is very close to the reanalysis data (Eqs. A2–A4). These results show that unlike LR-ESMs, the HR-ESMs are generally capable of reproducing the frequencies of the Loop Current north and south positions according to the relation of Maze et al (2015).

Temporal match

Data-model temporal agreement is the third validation task, which shows relatively large mismatch specifically with respect to LCS. The HR-ESMs multi-model ensemble
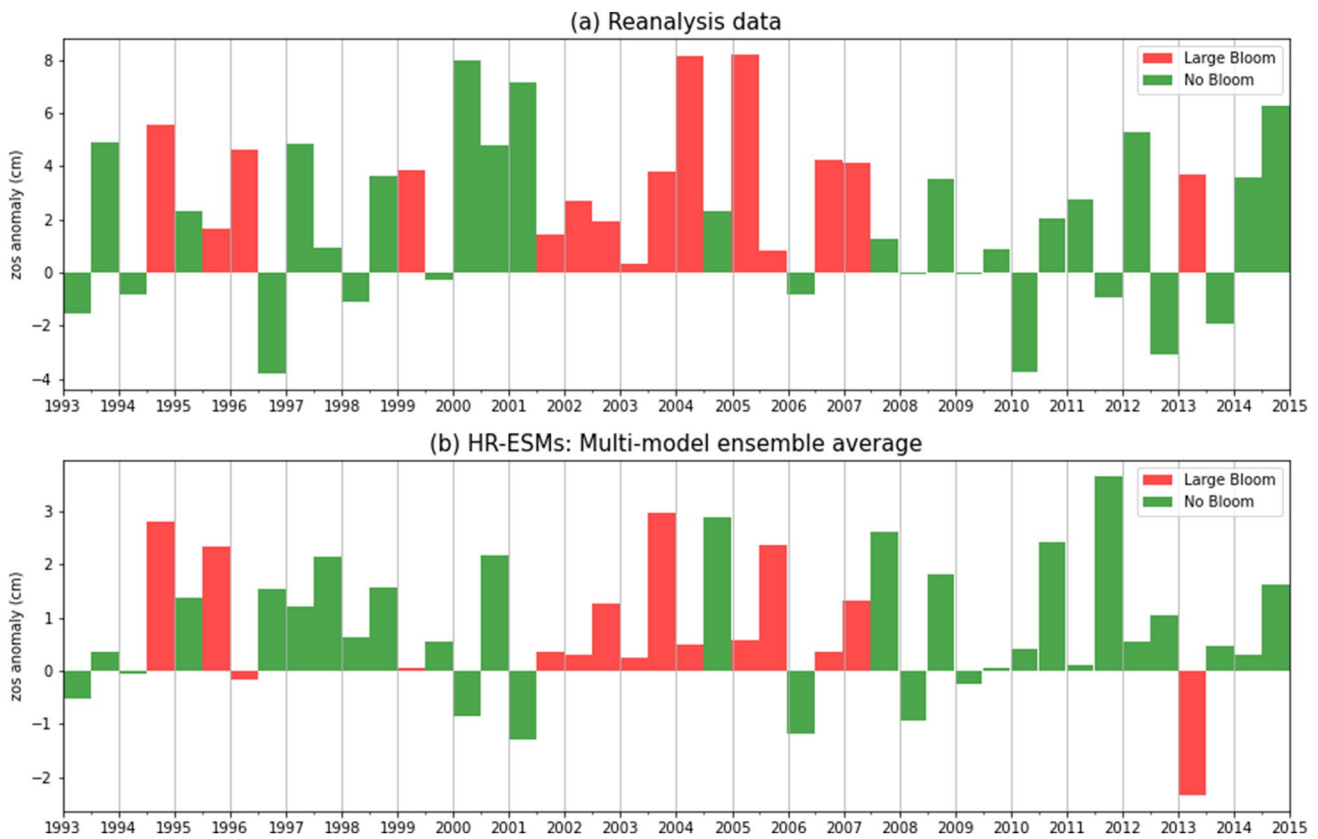
Fig. 3 Temporal match of large bloom/no bloom with Loop Current positions given by (**a**) observation reanalysis, and (**b**) simulations of HR-ESMs for multi-model ensemble average. Positive and negative bars indicate LCN and LCS, respectively

Table 2 Frequencies of LCN and LCS positions, and their relation to the occurrence of large blooms

Ensemble Average	Frequency		LCN		LCS		Temporal match		
	LCN	LCS	No-bloom	Large bloom	No-bloom	Large bloom	LCN	LCS	Total
Altimetry reanalysis data	32	12	17	15	12	0	32	12	44
Best single-model (ECMWF-IFS-MR)	33	11	21	12	8	3	26	5	31
HR-ESMs multi-model	35	9	22	13	7	2	28	5	33
LR-ESMs multi-model	0	44	0	0	29	15	0	12	12

Ensemble average refers to simple average of all model runs within the ensemble, with the exception of the reanalysis data that has only one realization

average has a total temporal match of 33 intervals out of 44. This means that during 44 intervals of the study period, the Loop Current position (i.e., LCN or LCS) of the model simulation matched that of the reanalysis data for 33 intervals, and for 11 intervals they were mismatching. Out of 32 intervals showing LCN by the reanalysis data, the model simulations matched 26 of them with an error of 18.75% (Eq. A6).

Out of the 12 intervals indicating LCS by the reanalysis data, the model simulations matched only five of them with an error of 58.33% (Eq. A5). In summary, the HR-ESMs multi-model ensemble average has a total temporal match error of 25% error as calculated from Table 2 (i.e., [44–33]/44 as shown by Eq. A7), and this error is more pronounced for the LCS than LCN. The error is invariant to the first year period

(i.e., Jan–Jun), and second year period (i.e., Jul–Dec). Out of the 15 large blooms, this error in the LCS has resulted in 2 false-positive periods of bloom formation that is 2 LCS intervals with large bloom (Eq. A8). In comparison, LR-ESM shows 15 false positives of bloom formation that is 15 LCS intervals with large bloom (Eq. A8).

Poor temporal match is expected. Given one year operational scale of ESMs (Chou et al. 2018), temporal mismatch for shorter intervals is expected due to weak signal-to-noise ratio in short-timescale predictions, systematic biases, and drifting. In addition, both the historical and hist-1950 experiments are free-running, which means that they are not expected to temporally coincide with real-world conditions. This can be particularly true for the historical simulations, which might be further out of synchronization with real conditions relative to hist-1950. This temporal match can even suffer from systematic bias over several decades. For example, Tokarska et al (2020) noted that for certain models (e.g., E3SM) the uncertainty in climate feedbacks and the aerosol forcing can result in historical warming similarly as observation, but with poor temporal agreement. This remark on simulated global mean surface air temperature may also be applicable for sea surface height. In other words, as no temporal match with historical record is generally expected, global predictions can be analyzed for processes and cycles, but not temporal alignment of specific ocean features. Accordingly, we attempt to find a coarse temporal agreement based on long interval (i.e., 6 month interval) using the coarse relationship of Maze et al. (2015) between Loop Current positions and red tide blooms. Thus, this task can be considered as pseudotemporal correspondence that captures the general pattern of a dynamic process. While temporal match is not critical for the main modeling purpose, which is to understand future trends and frequencies of red tide, it could have additional benefits such as using ESMs to develop an early warning system for red tide. ESMs are generally designed to make predictions at coarse time scales of decades to centuries. However, multiple techniques (e.g., downscaling, pattern scaling, and use of analogues) can be used to provide information at fine time horizons that match the decision contexts (van den Hurk et al. 2018). Additionally, coupled ESMs are now being tested for global prediction on short-range timescales (Brassington et al. 2015; Hewitt et al. 2017). These points are further discussed in "ESMs for regional environmental management" section.

Study findings and limitations

Several relationships have been established between Loop Current and red tide blooms (Weisberg et al. 2014, 2019; Maze et al. 2015; Liu et al. 2016a). The purpose of this work is not to support or refute any of these relations, but to use the empirical correlation of Maze et al. (2015) to illustrate the potential use of the publicly available data of CMIP6 for providing environmental services and to facilitate this discussion.

We illustrate data-model evaluation of Loop Current simulation using HR-ESMs for three basic tasks. First, adequate simulation of the spatial phenomena of interest is a bottleneck condition. According to Haarsma et al. (2016) to provide information relevant for stakeholders and adaptation strategies, regional climate information focuses on smaller scales and extreme events and requires high-resolution modeling to better capture local processes and teleconnections with distant regions that has a strong impact on the region of interest. For example, our case study shows the importance of simulating the regional phenomena of Loop Current that loops the Gulf of Mexico, which requires HR-ESMs versus a global phenomenon such as the Gulf Stream, which is a strong ocean current that circulate warm water from the Gulf of Mexico into the Atlantic Ocean. Unlike low-resolution ESMs, HR-ESMs can resolve the phenomena of interest at the regional scale (e.g., LCN and LCS) as suggested by other studies (Caldwell et al. 2019; Hoch et al. 2020). Being able to simulate the underlying physical processes of interest is a prerequisite to any meaningful ocean biogeochemical modeling at the regional scale.

Second, adequate estimation of the frequency of event oscillation (e.g., frequency of LCS and accordingly the absence of large blooms) is important for understanding the impacts of different climate scenarios on the frequency of red tide as explained below. Since LR-ESMs cannot simulate the physical phenomena of interest, this class of models failed to reproduce the observed frequency (Table 2).

Third, temporal matching at management timescale can permit additional services. Theoretically, the temporal correspondence obtained in this study could be a mere coincident. Otherwise, this could be attribute to the use heuristic relation with coarse temporal resolution. This might suggest that a pseudotemporal correspondence might be possible in the absence of a large drift. If such temporal correspondence cannot be established, this should not impact the main

modeling purpose of understanding the frequency and trend of red tide under different climate scenarios and of estimating the socioeconomic impacts accordingly. Such temporal correspondence is generally not currently possible without downscaling, and substantial long-term investment in climate science capability and model design are still needed to resolve finer spatiotemporal scales (Fiedler et al. 2021). However, if temporal match with ocean observations at short timescale is required, strategies to reduce mismatch include improving initial conditions (Hewitt et al. 2017), bias correction and recalibration methods (Manzanas 2020), and pattern scaling (van den Hurk et al. 2018). These can be simpler techniques compared to the more challenging dynamical downscaling techniques. In addition, this analysis can be repeated by replacing the CMIP6 data with CORDEX data as soon as they become available.

This study supports the evidence that improved horizontal resolution with weather-resolving global model resolutions (~25 km or finer) and using coupled ESMs (i.e., coupled simulations of atmosphere–cryosphere–land–ocean) can improve predictive performance at short timescales (Scaife et al. 2011, 2019; Hewitt et al. 2017; Little et al. 2019). While the focus of this study is the ocean component, the results are based on coupled simulations. By better capturing transient mesoscale motions, these simulations correspond to the observed ocean phenomena exhibiting fine scale boundary currents, transient fluctuations, coastal upwelling zones, meanders and jets (Hewitt et al. 2017), which can permit these models to be used for environmental management.
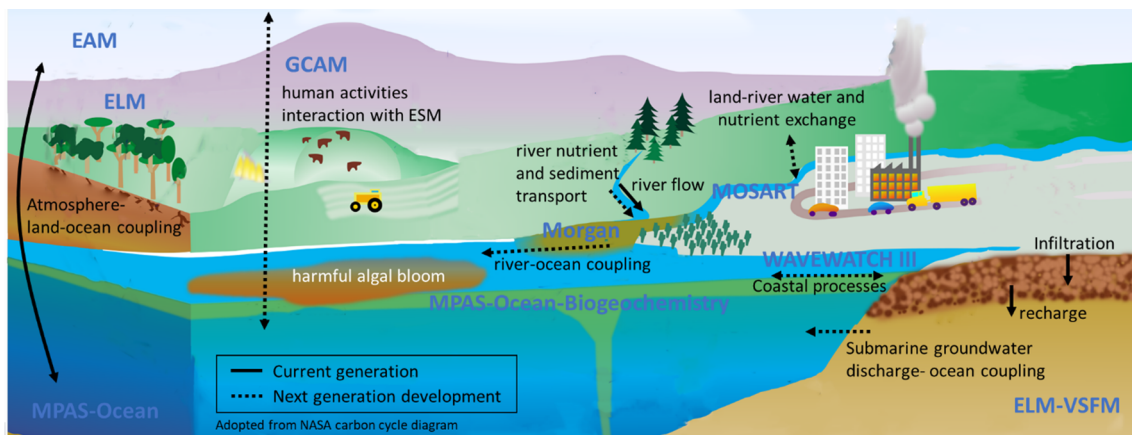
This study is a preliminary showcase of the possibility of using CMIP6 data for red tide management, and many further steps are needed. The presented results are mainly for preliminary validation of CMIP6 data, but are of limited use for predicting red tide in the Gulf of Mexico. With respect to the relationship between Loop Current and red tide, the only relation that we consider is that large blooms are unlikely to occur for the case of LCS (Maze et al. 2015). For the case of LCN, further relations (Weisberg et al. 2014, 2019; Liu et al. 2016a) are needed to constrain the cases of large and no blooms, respectively. In addition to Loop Current, other relevant drivers (e.g., African Sahara dust, offshore and alongshore wind speed, atmospheric CO_2 concentration, sea surface temperature, etc.) will be considered under different SSPs of CMIP6 in which socio-economic scenarios are used to derive emissions scenarios with and without climate polices for mitigation. These drivers may be simultaneously considered using machine learning in a probability framework in a future study. For example, Tonelli

et al. (2021) used machine learning with CMIP6 data to study marine microbial communities under different future scenarios. While the abovementioned drivers of red tide can be mostly assessed with CMIP6 data, several limitations persist as discussed next.

ESMs for regional environmental management

Limitations and prospects of ESMs for regional environmental management

While the presented case study is on red tide, ESMs can be used to provide multiple environmental management services that are controlled by land to ocean nutrient and sediment transport, land and ocean biogeochemical reactions, tropical cyclones, and wind speed and direction. To illustrate this potential use of HR-ESMs in providing environmental management services, we discuss the outputs of ESMs that are useful for red tide management, which can be generalized to other regional environmental problems. Brand and Compton (2007) discussed different drivers that contribute to the initiation, growth, maintenance, and termination of red tide. Box 1 summarizes these drivers with their corresponding ESMs outputs, using the Energy Exascale Earth System Model (E3SM) as an example. The E3SM project is an ongoing state-of-the-art Earth system modeling project that attempts to answer more demanding questions related to human activities interaction with the Earth system. Physical ocean and atmospheric processes presented in Box 1 are already implemented in current generation of HR-ESMs. River flow will be available for HR-ESMs, yet river nutrient transport and simulation of anthropogenic impacts will be addressed in next generation development (Leung et al. 2020). With respect to the ocean biogeochemical processes (e.,g., Heil et al., 2014), the implementation of the biogeochemical processes presented in Box 1 in HR-ESMs is still in progress. However, biogeochemical cycles are not yet coupled between ocean and land in the current generation development. The feedbacks between the ocean biogeochemistry and the physical ocean and climate states, transport of nitrogen and phosphorus from land to ocean, and river–ocean biogeochemistry fluxes, and the incorporation of anthropogenic nutrient sources at a regional scale are ongoing in E3SM project (Burrows et al. 2020; Leung et al. 2020).

Drivers of red tide	Corresponding ESM components and outputs
Ocean-physics Increase in ocean water temperature and change in water mass structure may increase *K. brevis* occurrence	**MPAS-Ocean** Sea surface temperature and sea surface salinity
Atmosphere-ocean-physics Tropical cyclones of North Atlantic Oscillation, Atlantic Multi-decadal Oscillation, and hurricane activities affect the population dynamics.	**EAM-MPAS-Ocean** Sea level pressure, air temperature, and wind speed outputs using a feature tracking software to detect tropical cyclones vortices.
Land-river-sediment-ocean River flow, and nutrient and sediment transport from rivers to coastal water control the spatial and temporal extend of *K. brevis* blooms.	**EAM-MOSART- Morgan-MPAS-Ocean** River flow-transport simulation using MOSART including water exchange with the atmosphere and land, and sediment transport using Morgan are active research areas (Tan et al. 2020, 2021) for next generation development.
Land-groundwater-ocean Submarine groundwater discharge is a nutrient source for *K. brevis*. And changes the biogeochemical and physical properties of the ocean water	**EAM-VSFM-MPAS-Ocean** Variably saturated flow model (VSFM, Bisht *et al* 2018) solves a tightly coupled multi-component problem (e.g., transport of water and solutes through the soil-plant-atmosphere continuum) with fully coupled conservation of mass and energy equations in the subsurface.
Ocean-biogeochemistry Natural and anthropogenic nutrients that are nitrogen and phosphorus from non-point sources in estuarine, coastal, and offshore regions such as estuarine flux, benthic flux, atmospheric deposition, pelagic nitrogen fixation by *Trichodesmium* and other groups, biomass decay, photochemical nutrient production, zooplankton excretion, microzooplankton grazing, mixotrophic consumption of picoplankton, and nitrification (Heil et al. 2014) support *K. brevis* blooms .	**MPAS-Ocean-Biogeochemistry** Simulating upper ocean ecological and full-depth biogeochemical dynamics with multiple phytoplankton functional groups (e.g., diatoms, diazotrophs, small phytoplankton, and Phaeocystis), zooplankton, dimethyl sulfide production, multiple pools of dissolved organic matter and limiting nutrients (e.g., nitrate, ammonium, phosphate, silicate, and iron), and inorganic carbonate chemistry (Burrows et al. 2020; Jeffery et al. 2020).

Box 1

Drivers of red tide and corresponding ESM components and outputs for the current and future generation development using E3SM as example. E3SM components include E3SM atmospheric model (EAM), E3SM land model (ELM), subsurface variably saturated flow model (ELM-VSFM, Bisht et al. 2018), river model (MOSART), sediment model (Morgan, Tan et al. 2020, 2021), ocean model (MPAS-Ocean), ocean biogeochemistry model (MPAS-Ocean-Biogeochemistry), costal processes model (WAVEWATCH III), and global change analysis model (GCAM) for human activities.

The ongoing development of Earth system observations and modeling will allow for the ESMs to provide adequate environmental management services useful to the society. Many of the current model products suffer from missing anthropogenic impacts on the environment and full coupling of river, land, ocean, and atmospheric biogeochemistry. Such coupling along with improved model fidelity is an active research field in Earth system modeling. In addition, the need to increase model fidelity is apparent. For example, accounting for storm surges and coastal processes to simulate regional sea-level rise and coastal inundation is required for providing multiple regional environmental management services (Ward et al. 2020; Brus et al. 2021), including better simulation of Loop Current for red tide management. In addition to biogeophysical processes, interactions between natural systems and human activities, which include human behaviors and socioeconomic systems, require carefully assessing interdisciplinary efforts with respect to emerging applications of ESMs (Calvin and Bond-Lamberty 2018; Donges et al. 2020; Beckage et al. 2020). The current generation of ESMs represents human activities by considering landcover and landuse change, and through macroeconomic integrated assessment models with a typical limited scope (Donges et al. 2020). Coupling between human activities and ESMs (Monier et al. 2018), which is an ongoing development effort by several modeling groups (Leung et al. 2020; Kawamiya et al. 2020), shall open avenues for multiple environmental management services. For example, the E3SM project efforts on coupling land and river components with a crop model will better represent the impacts of crop and water management on streamflow and temperature, floodplain inundation, and river biogeochemistry (Leung et al. 2020).

Approaches for using ESMs in regional environmental management

There are several approaches for using ESMs to advance scientific understanding and to manage regional environmental problems. Taking red tide as an example, the first approach is to add the *K. brevis* phytoplankton functional group to the ocean biogeochemical component of the ESM to develop an ecosystem-based model to simulate red tide online as the ESM simulation is running. For example, Jeffery et al (2020) investigated the controls on sea ice algal production in the Artic using E3SM. However, for this first approach regional ESM model is required as global EMS is computationally expensive. For example, Reale et al (2020) showed the potential of using a regional ESM as a suitable tool for the analysis of the impacts of climate change on marine biogeochemistry in the Mediterranean region. The second approach in Box 2 is to develop a mechanistic model (e.g., a Lagrangian model) to simulate red tides off-line given the ESMs simulation outputs of CMIP6, CORDEX, etc. The third approach, which seems to have vast potentials, is to use the outputs of ESMs to develop a phenomenological model (e.g., a machine learning model) to predict red tide off-line. Box 2 lists the advantages and disadvantages of these three approaches, which are not mutually exclusive and can leverage on one another.

Add the processes of interest to the ESM

Task: Add *K. brevis* phytoplankton functional group to the ocean biogeochemical component of the ESM
Modeling effort and time: Relatively large

Example:	Advantages
• regional ESM that functions as an ecosystem-based model	• simulate the process of interest (e.g., *K. brevis* blooms) in a coupled ESM simulation
	Disadvantages
	• developing a regional ESM using dynamical downscaling is a formidable modeling task
	• less autonomy over the model and predication skill can be low
	• high computational cost

Develop a mechanistic model using (global or regional) ESM outputs

Task: Select outputs of the ESM that correspond to red tide drivers as needed to develop a mechanistic model
Modeling effort and time: Intermediate to large depending on the processes of interest and leveraging on exiting codes

Example:	Advantages
• Lagrangian model	• simulate the process of interest (e.g., *K. brevis* blooms)
• ecosystem-based model	• more autonomy over the model development, parameterization, and calibration
• Individual-based model	Disadvantages
	• ESM outputs need to be validated
	• limited number of processes can only be considered as mechanistic incorporation of more processes can render the model cumbersome

Develop a phenomenological model using (global or regional) ESM outputs

Task: Select outputs of the ESM that correspond to red tide drivers as need to develop the phenomenological model
Modeling effort and time: Small to intermediate depending on the number of the processes of interest

Example:	Advantages
• machine learning model	• many external perturbations that are reliable indicators of ecosystem functioning can be easily considered
• statistical model	• discover causal interdependencies of the underlying drivers
• system dynamics model	Disadvantages
• risk-based model	• ESM outputs need to be validated
	• inferring physical insights may not be straightforward

Box 2

Approaches of using ESMs for regional environmental management with red tide as an example.

Collaborative modeling

To extend the practical applications of ESMs to inform societal actions, stakeholder participation plays an important role in the development of ESMs. This aspect of climate services still calls for more attention (Bojovic et al. 2021). Beyond providing understanding of the climate system, ESMs essentially aim at providing climate services that meet the strong societal demand for salient and credible scientific information to improve the society's resilience and risk management to climate-related hazards (Hewitt et al. 2012; Eyring et al. 2019). Stakeholder participation is part of the bilateral process that adds saliency, credibility, and legitimacy (Cash et al. 2002) to the products of ESMs. On the one hand, high-quality simulations, and accordingly deeper scientific understanding of regional Earth system processes, provide stakeholders with the information to guide societal decision-making with respect to regional environmental management. On the other hand, a dialog between the ESM developers and environmental managers is needed to improve the use of ESMs and the direction of ESMs development (Gutowski et al. 2020). This includes meeting the space and timescale requirements, coupling of land, river and ocean, and inclusion of anthropogenic impacts and human activities to user requirements with respect to real-world applications. In addition, participation should extend from mere coordination to provide demand-driven services, to participatory modeling with consultation and discussion, and further to collaborative modeling with co-design (Basco-Carrera et al. 2017) to provide tailored regional models and services. For example, the development of interactively coupled regional ESMs is one of the main future directions of regional climate research (Giorgi and Gao 2018). For developing and running regional ESM simulations targeting environmental problems, collaborative modeling between ESM projects and environmental agencies is indispensable.

Conclusions

This article discusses the potential uses of the HR-ESMs of CMIP for environmental management at regional scale. We present a case study about harmful algae blooms in Florida commonly known as red tide, and the position of Loop Current, which is a warm ocean current that enters the Gulf of Mexico, can be the first predictor of red tide. This case study was intended to tailor the outputs of CMIP6 models to an environmental application at the regional scale. Three basic criteria for evaluating model predictions have been presented. Unlike LR-ESMs, HR-ESMs can adequately simulate the physical phenomena of interest (i.e., Loop Current

position), which is prerequisite to any meaningful biogeochemical modeling. In addition, HR-ESMs can adequately reproduce the frequency of the event of interest (i.e., LCN and LCS), which is crucial for assessing the impact of climate change on red tide. At last, the most challenging evaluation task is the temporal agreement of model simulations with observation data at the management timescale. Large temporal mismatch is observed suggesting that this is an unsuitable criterion for evaluating global ESMs. Loop Current position alone is only one predictor. Machine learning seems to be a viable option for prediction using additional Loop Current relations and red tide drivers. The article also identifies the current gaps and development needs of ESMs with respect to environmental management services, while realizing that the new generation of HR-ESMs in CMIP6 is a remarkable development. The development gaps include (1) coupling of land, river, and ocean biogeochemistry, (2) accounting of anthropogenic disturbances on natural systems (e.g., anthropogenic nutrient sources and freshwater withdrawal), (3) coupling between human activities and ESMs, and (4) advancement of interactive coupled regional ESMs. Such developments are needed for red tide management, and many other environmental management services. Stakeholder engagement in model development is essential to facilitate the translation of scientific understanding to better inform decision-making of regional environmental management.

Appendix

We process zos data to determine Loop Current position (i.e., LCN and LCS) to obtain the zos anomaly per time interval

$$h_t = \max_{h_{t,n}} \left(\underset{m}{\triangle} \left[\underset{l}{E} \left[\underset{k}{E} \left[\underset{j}{E} \left(h_{t,n,m,l,k,j} | M_k \right) \right] \right] \right] \right) \tag{A1}$$

such that the expectations $\underset{j}{E}$, $\underset{k}{E}$ and $\underset{l}{E}$ of zos data are taken for all model runs with index j of each ensemble member M_k, all ensemble members M_k with index k, and all data points with index l along each segment (i.e., north and south segments in Fig. 1b), respectively. Then the difference $\underset{m}{\triangle}$ between the north and south segments with index $m \in [1, 2]$ is taken resulting in $h_{t,n}$ with $n \in [1, 6]$ because we have monthly zos data, and we use 6-month interval. Finally, for each of the 6-month intervals t starting from 1993 to 2015, the maximum $h_{t,n}$ is selected resulting in zos anomaly values h_t such that $t \in [1, 44]$. There are 44 h_t values because we use a 6-month interval (i.e., half a year) and given the 22-year study period. As the Loop Current position is a cycling event, taking the maximum value $\underset{h_{t,n}}{max}(.)$ in each time inter-

val is more robust than the average value that may dilute the signals of the LCS.

To evaluate the predictive performance and compare the model results and reanalysis data we use the following four metrics:

Loop Current position ratio (y_1): This is the ratio of the frequency of LCS to LCN.

$$y_1 = \frac{\sum_{t=1}^{T} H_{LCS}(h_t)}{\sum_{t=1}^{T} H_{LCN}(h_t)} \tag{A2}$$

such that $\sum_{t=1}^{T} H_{LCS}(h_t)$ and $\sum_{t=1}^{T} H_{LCN}(h_t)$ are the count of LCS and LCN intervals given the total number of intervals $T = 44$, with indicator function for LCS.

$$H_{LCS}(h_t) = \begin{cases} 1, & h_t \geq 0 \\ 0, & h_t < 0 \end{cases} \tag{A3}$$

and LCN

$$H_{LCN}(h_t) = \begin{cases} 1, & h_t < 0 \\ 0, & h_t \geq 0 \end{cases} \tag{A4}$$

Temporal match error (y_2): For reanalysis data and model predictions, the temporal match with respect to LC position for LCS.

$$y_{2,LCS} = \frac{\sum_{t=1}^{T} H_{LCS}(h_{t,obs}) - \sum_{t=1}^{T} (h_{t,obs} < 0 \wedge h_t < 0)}{\sum_{t=1}^{T} H_{LCS}(h_{t,obs})} \tag{A5}$$

for LCN.

$$y_{2,LCN} = \frac{\sum_{t=1}^{T} H_{LCN}(h_{t,obs}) - \sum_{t=1}^{T} (h_{t,obs} \geq 0 \wedge h_t \geq 0)}{\sum_{t=1}^{T} H_{LCN}(h_{t,obs})} \tag{A6}$$

and both positions.

$$y_2 = \frac{T - \sum_{t=1}^{T} (h_{t,obs} \geq 0 \wedge h_t \geq 0) - \sum_{t=1}^{T} (h_{t,obs} < 0 \wedge h_t < 0)}{T} \tag{A7}$$

where $\sum_{t=1}^{T} H_{LCS}(h_{t,obs})$ and $\sum_{t=1}^{T} H_{LCN}(h_{t,obs})$ are for reanalysis data $h_{t,obs}$(Eq. A1). In Eqs. A5–7, $\sum_{t=1}^{T} (h_{t,obs} \geq 0 \wedge h_t \geq 0)$ and $\sum_{t=1}^{T} (h_{t,obs} < 0 \vee h_t < 0)$ present the temporal match counts of reanalysis data and model simulation for LCS and LCN, respectively. The logical conjunction $\wedge$ of $(h_{t,obs} \geq 0 \wedge h_t \geq 0)$, for example, yields one when $h_{t,obs} \geq 0$ and $h_t \geq 0$ are both true, and yields zero otherwise.

K. brevis error (y_3): When LCS coincides with a large bloom, this is a false-negative prediction of red tide.

$$y_3 = \frac{\sum_{t=1}^{T} (h_t < 0 \wedge H(z_t) = 1)}{N_{bloom}} \tag{A8}$$

where $H(z_t)$ is an indicator function with zero and one for no bloom and large bloom and, respectively, and N_{bloom} is the number of large-bloom.

Declarations

Conflict of interest The authors have not disclosed any conflict of interest.

References

Adachi SA, Tomita H (2020) Methodology of the constraint condition in dynamical downscaling for regional climate evaluation: a review. J Geophys Res Atmos. https://doi.org/10.1029/2019JD032166

Ahmed SM (2021) Modeling crop yields amidst climate change in the Nile basin (2040–2079). Model Earth Syst Environ. https://doi.org/10.1007/s40808-021-01199-0

Basco-Carrera L, Warren A, van Beek E et al (2017) Collaborative modelling or participatory modelling? A framework for water resources management. Environ Model Softw 91:95–110. https://doi.org/10.1016/j.envsoft.2017.01.014

Beckage B, Lacasse K, Winter JM et al (2020) The Earth has humans, so why don't our climate models? Clim Change 163:181–188. https://doi.org/10.1007/s10584-020-02897-x

Bisht G, Riley WJ, Hammond GE, Lorenzetti DM (2018) Development and evaluation of a variably saturated flow model in the global E3SM land model (ELM) version 1.0. Geosci Model Dev 11:4085–4102. https://doi.org/10.5194/gmd-11-4085-2018

Bojovic D, St Clair AL, Christel I et al (2021) Engagement, involvement and empowerment: Three realms of a coproduction framework for climate services. Glob Environ Change 68:102271. https://doi.org/10.1016/j.gloenvcha.2021.102271

Brand LE, Compton A (2007) Long-term increase in Karenia brevis abundance along the Southwest Florida Coast. Harmful Algae 6:232–252. https://doi.org/10.1016/j.hal.2006.08.005

Brassington GB, Martin MJ, Tolman HL et al (2015) Progress and challenges in short- to medium-range coupled prediction. J Oper Oceanogr 8:s239–s258. https://doi.org/10.1080/1755876X.2015.1049875

Brus SR, Wolfram PJ, Van Roekel LP, Meixner JD (2021) Unstructured global to coastal wave modeling for the energy exascale earth system model using WAVEWATCH III version 6.07. Geosci Model Dev 14:2917–2938. https://doi.org/10.5194/gmd-14-2917-2021

Burrows SM, Maltrud M, Yang X et al (2020) The DOE E3SM v1.1 biogeochemistry configuration: description and simulated ecosystem-climate responses to historical changes in forcing. J Adv Modeling Earth Syst. https://doi.org/10.1029/2019MS001766

Caldwell PM, Mametjanov A, Tang Q et al (2019) The DOE E3SM coupled model version 1: description and results at high resolution. J Adv Modeling Earth Syst 11:4095–4146. https://doi.org/10.1029/2019MS001870

Calvin K, Bond-Lamberty B (2018) Integrated human-earth system modeling—state of the science and future directions. Environ Res Lett 13:063006. https://doi.org/10.1088/1748-9326/aac642

Cash D, Clark WC, Alcock F et al (2002) Salience, credibility, legitimacy and boundaries: linking research. Assessment and Decision Making, Social Science Research Network, Rochester, NY

Chou J, Hu C, Dong W, Ban J (2018) Temporal and spatial matching in human-earth system model coupling. Earth Space Sci 5:231–239. https://doi.org/10.1002/2018EA000371

Dixon AM, Forster PM, Beger M (2021) Coral conservation requires ecological climate-change vulnerability assessments. Front Ecol Environ n/a: https://doi.org/10.1002/fee.2312

Donges JF, Heitzig J, Barfuss W et al (2020) Earth system modeling with endogenous and dynamic human societies: the copan:core open World-Earth modeling framework. Earth Syst Dyn 11:395–413. https://doi.org/10.5194/esd-11-395-2020

Drévillon M, Régnier C, Lellouche J-M, et al (2018) Quality Information Document For products GLOBAL-REANALYSIS-PHY-001-030, Ref :CMEMS-GLO-QUID-001-030

Elshall AS (2021) Data of Earth system models for regional environmental management: prospects and limitations of the current generation of CMIP6 and next generation development. https://doi.org/10.5281/zenodo.4556311

Eyring V, Bony S, Meehl GA et al (2016) Overview of the coupled model intercomparison project phase 6 (CMIP6) experimental design and organization. Geosci Model Dev 9:1937–1958. https://doi.org/10.5194/gmd-9-1937-2016

Eyring V, Cox PM, Flato GM et al (2019) Taking climate model evaluation to the next level. Nature Clim Change 9:102–110. https://doi.org/10.1038/s41558-018-0355-y

Fernandez E, Lellouche JM (2018) Product user manual For the Global Ocean physical reanalysis product GLOBAL_REANALYSIS_ PHY_001_030. 15

Fiedler T, Pitman AJ, Mackenzie K et al (2021) Business risk and the emergence of climate analytics. Nat Clim Chang 11:87–94. https://doi.org/10.1038/s41558-020-00984-6

FWRI (2020) HAB monitoring database. In: Florida fish and wildlife conservation commission. http://myfwc.com/research/redtide/monitoring/database/. Accessed 23 Dec 2020

Giorgi F, Gao X-J (2018) Regional earth system modeling: review and future directions. Atmos Ocean Sci Letters 11:189–197. https://doi.org/10.1080/16742834.2018.1452520

Golaz J-C, Caldwell PM, Roekel LPV et al (2019) The DOE E3SM coupled model version 1: overview and evaluation at standard resolution. J Adv Modeling Earth Syst 11:2089–2129. https://doi.org/10.1029/2018MS001603

Gutowski WJ Jr, Giorgi F, Timbal B et al (2016) WCRP coordinated regional downscaling experiment (CORDEX): a diagnostic MIP for CMIP6. Geosci Model Dev 9:4087–4095. https://doi.org/10.5194/gmd-9-4087-2016

Gutowski WJ, Ullrich PA, Hall A et al (2020) The ongoing need for high-resolution regional climate models: process understanding and stakeholder information. Bull Am Meteor Soc 101:E664–E683. https://doi.org/10.1175/BAMS-D-19-0113.1

Haarsma RJ, Roberts MJ, Vidale PL et al (2016) High resolution model intercomparison project (HighResMIP v1.0) for CMIP6. Geosci Model Dev 9:4185–4208. https://doi.org/10.5194/gmd-9-4185-2016

Haarsma R, Acosta M, Bakhshi R et al (2020) HighResMIP versions of EC-Earth: EC-Earth3P and EC-Earth3P-HR – description, model computational performance and basic validation. Geosci Model Dev 13:3507–3527. https://doi.org/10.5194/gmd-13-3507-2020

Heil CA, Dixon LK, Hall E et al (2014) Blooms of Karenia brevis (Davis) G. Hansen & Ø. Moestrup on the West Florida shelf: nutrient sources and potential management strategies based on a multi-year regional study. Harmful Algae 38:127–140. https://doi.org/10.1016/j.hal.2014.07.016

Hewitt C, Mason S, Walland D (2012) The global framework for climate services. Nat Clim Chang 2:831–832. https://doi.org/10.1038/nclimate1745

Hewitt HT, Bell MJ, Chassignet EP et al (2017) Will high-resolution global ocean models benefit coupled predictions on short-range to climate timescales? Ocean Model 120:120–136. https://doi.org/10.1016/j.ocemod.2017.11.002

Hoch KE, Petersen MR, Brus SR et al (2020) MPAS-ocean simulation quality for variable-resolution north american coastal meshes. J Adv Modeling Earth Syst. https://doi.org/10.1029/2019MS001848

Iles CE, Vautard R, Strachan J et al (2020) The benefits of increasing resolution in global and regional climate simulations for European climate extremes. Geosci Model Dev 13:5583–5607. https://doi.org/10.5194/gmd-13-5583-2020

Ilori OW, Balogun IA (2021) Evaluating the performance of new CORDEX-Africa regional climate models in simulating West African rainfall. Model Earth Syst Environ. https://doi.org/10.1007/s40808-021-01084-w

Jeffery N, Maltrud ME, Hunke EC et al (2020) Investigating controls on sea ice algal production using E3SMv1.1-BGC. Ann Glaciol 61:51–72. https://doi.org/10.1017/aog.2020.7

Jiaxiang G, Shoshiro M, Roberts MJ et al (2020) Influence of model resolution on bomb cyclones revealed by HighResMIP-PRIMAVERA simulations. Environ Res Lett 15:084001. https://doi.org/10.1088/1748-9326/ab88fa

Joussaume S, Lawrence B, Guglielmo F (2017) Update of the ENES infrastructure strategy, 2012-2022, ENES Report Series 2, 20 pp. https://portal.enes.org/community/about-enes/the-future-ofenes/ENES_strategy_update_2017.pdf. Accessed 7 April 2022

Kawamiya M, Hajima T, Tachiiri K et al (2020) Two decades of earth system modeling with an emphasis on model for interdisciplinary research on climate (MIROC). Prog Earth Planet Sci 7:64. https://doi.org/10.1186/s40645-020-00369-5

Le T, Ha K-J, Bae D-H, Kim S-H (2020) Causal effects of Indian Ocean Dipole on El Niño-Southern Oscillation during 1950–2014 based on high-resolution models and reanalysis data. Environ Res Lett. https://doi.org/10.1088/1748-9326/abb96d

Leung LR, Bader DC, Taylor MA, McCoy RB (2020) An introduction to the E3SM special collection: goals, science drivers, development, and analysis. J Adv Modeling Earth Syst. https://doi.org/10.1029/2019ms001821

Little CM, Hu A, Hughes CW et al (2019) The Relationship between U.S. East Coast Sea Level and the Atlantic Meridional overturning circulation: a review. J Geophysical Res: Oceans 124:6435–6458. https://doi.org/10.1029/2019JC015152

Liu J, Fang S (2017) Comprehensive evaluation of the potential risk from cyanobacteria blooms in Poyang Lake based on nutrient zoning. Environ Earth Sci 76:342. https://doi.org/10.1007/s12665-017-6678-6

Liu Y, Weisberg RH, Lenes JM et al (2016a) Offshore forcing on the "pressure point" of the West Florida Shelf: anomalous upwelling and its influence on harmful algal blooms. J Geophysical Res: Oceans 121:5501–5515. https://doi.org/10.1002/2016JC011938

Liu Y, Weisberg RH, Vignudelli S, Mitchum GT (2016b) Patterns of the loop current system and regions of sea surface height

variability in the eastern Gulf of Mexico revealed by the self-organizing maps. J Geophysical Res: Oceans 121:2347–2366. https://doi.org/10.1002/2015JC011493

Manzanas R (2020) Assessment of model drifts in seasonal forecasting: sensitivity to ensemble size and implications for bias correction. J Adv in Modeling Earth Syst. https://doi.org/10.1029/2019MS001751

Maze G, Olascoaga MJ, Brand L (2015) Historical analysis of environmental conditions during Florida Red Tide. Harmful Algae 50:1–7. https://doi.org/10.1016/j.hal.2015.10.003

Monier E, Paltsev S, Sokolov A et al (2018) Toward a consistent modeling framework to assess multi-sectoral climate impacts. Nat Commun 9:660. https://doi.org/10.1038/s41467-018-02984-9

Perkins S (2019) Inner workings: ramping up the fight against Florida's red tides. PNAS 116:6510–6512. https://doi.org/10.1073/pnas.1902219116

Reale M, Giorgi F, Solidoro C et al (2020) The regional earth system model RegCM-ES: evaluation of the mediterranean climate and marine biogeochemistry. J Adv Modeling Earth Syst. https://doi.org/10.1029/2019MS001812

Riahi K, van Vuuren DP, Kriegler E et al (2017) The Shared socioeconomic pathways and their energy, land use, and greenhouse gas emissions implications: an overview. Glob Environ Chang 42:153–168. https://doi.org/10.1016/j.gloenvcha.2016.05.009

Roberts CD, Senan R, Molteni F et al (2018a) Climate model configurations of the ECMWF integrated forecasting system (ECMWF-IFS cycle 43r1) for HighResMIP. Geosci Model Dev 11:3681–3712. https://doi.org/10.5194/gmd-11-3681-2018

Roberts MJ, Vidale PL, Senior C et al (2018b) The Benefits of global high resolution for climate simulation: process understanding and the enabling of stakeholder decisions at the regional scale. Bull Am Meteor Soc 99:2341–2359. https://doi.org/10.1175/BAMS-D-15-00320.1

Roberts MJ, Baker A, Blockley EW et al (2019) Description of the resolution hierarchy of the global coupled HadGEM3-GC3.1 model as used in CMIP6 HighResMIP experiments. Geosci Model Dev 12:4999–5028. https://doi.org/10.5194/gmd-12-4999-2019

Scaife AA, Copsey D, Gordon C et al (2011) Improved Atlantic winter blocking in a climate model. Geophys Res Lett. https://doi.org/10.1029/2011GL049573

Scaife AA, Camp J, Comer R et al (2019) Does increased atmospheric resolution improve seasonal climate predictions? Atmos Sci Lett 20:e922. https://doi.org/10.1002/asl.922

Sein DV, Mikolajewicz U, Gröger M et al (2015) Regionally coupled atmosphere-ocean-sea ice-marine biogeochemistry model ROM: 1. Description and validation. J Adv in Modeling Earth Syst 7:268–304. https://doi.org/10.1002/2014MS000357

Sturges W, Evans JC (1983) On the variability of the loop current in the Gulf of Mexico. J Mar Res 41:639–653. https://doi.org/10.1357/002224083788520487

Tan Z, Leung LR, Li H-Y et al (2020) A substantial role of soil erosion in the land carbon sink and its future changes. Glob Change Biol 26:2642–2655. https://doi.org/10.1111/gcb.14982

Tan Z, Leung LR, Li H-Y et al (2021) Increased extreme rains intensify erosional nitrogen and phosphorus fluxes to the northern Gulf of Mexico in recent decades. Environ Res Lett 16:054080. https://doi.org/10.1088/1748-9326/abf006

Tian R, An J (2013) Relationship between aerosol transport routes and red tide occurrences in the East China Sea. Environ Earth Sci 69:1499–1508. https://doi.org/10.1007/s12665-012-1984-5

Tokarska KB, Stolpe MB, Sippel S et al (2020) Past warming trend constrains future warming in CMIP6 models. Sci Adv. https://doi.org/10.1126/sciadv.aaz9549

Tonelli M, Signori CN, Bendia A et al (2021) Climate projections for the Southern Ocean reveal impacts in the marine microbial communities following increases in sea surface temperature. Front Mar Sci 8:636226. https://doi.org/10.3389/fmars.2021.636226

Usta DFB, Teymouri M, Chatterjee U, Koley B (2021) Temperature projections over Iran during the twenty-first century using CMIP5 models. Model Earth Syst Environ. https://doi.org/10.1007/s40808-021-01115-6

van den Hurk B, Hewitt C, Jacob D et al (2018) The match between climate services demands and Earth system models supplies. Clim Serv 12:59–63. https://doi.org/10.1016/j.cliser.2018.11.002

Ward ND, Megonigal JP, Bond-Lamberty B et al (2020) Representing the function and sensitivity of coastal interfaces in Earth system models. Nat Commun 11:2458. https://doi.org/10.1038/s41467-020-16236-2

Weisberg RH, Zheng L, Liu Y et al (2014) Why no red tide was observed on the West Florida continental shelf in 2010. Harmful Algae 38:119–126. https://doi.org/10.1016/j.hal.2014.04.010

Weisberg RH, Liu Y, Lembke C et al (2019) The coastal ocean circulation INFLUENCE on the 2018 West Florida Shelf K. brevis Red Tide Bloom. J Geophys Res: Oceans 124:2501–2512. https://doi.org/10.1029/2018JC014887

Wen S, Song L, Long H et al (2013) Nutrient-based method for assessing the hazard degree of red tide: a case study in the Zhejiang coastal waters, East China Sea. Environ Earth Sci 70:2671–2678. https://doi.org/10.1007/s12665-013-2324-0

Xu Y, Cheng C, Zhang Y, Zhang D (2014) Identification of algal blooms based on support vector machine classification in Haizhou Bay, East China Sea. Environ Earth Sci 71:475–482. https://doi.org/10.1007/s12665-013-2455-3